Using Topological Rearrangements to Characterize De-mixed Liquid Phases in Bio-membranes

Sahithya S. Iyer, Madhusmita Tripathy and Anand Srivastava

Molecular Biophysics Unit, Indian Institute of Science Bangalore, India

Abstract

Lateral heterogeneities in bio-membranes play a crucial role in various physiological functions of the cell. Such heterogeneities lead to demixing of lipid constituents and formation of distinct liquid domains in the membrane. We study lateral heterogeneities in terms of the topological rearrangements of lipids, to identify liquid-liquid phase co-existence in model membranes. By quantifying the degree of non-affineness associated with individual lipid, we are able to characterize the liquid ordered (L_o) and liquid disordered (L_d) phases in model lipid bilayers, without any prior knowledge on chemical identity of the lipids. We explore the usage of this method on all atom and coarse-grained lipid bilayer trajectories. This method is helpful in defining the instantaneous L_o-L_d domain boundaries in complex multi-component bilayer systems. The characterization can also highlight the effect of line-active molecules on the phase boundaries and domain mixing. Overall, we propose a framework to explore the molecular origin of spatial and dynamical heterogeneity in bio-membranes systems, which can not only be exploited in computer simulation, but also in experiments.

1 Introduction

Plasma membrane is a complex self-assembly of a variety of lipids, sterols and proteins. Differential molecular interactions among these diverse constituents gives rise to dynamic lateral heterogeneities in the membrane structure [1, 2]. Such heterogeneities lead to phase separation of the membrane constituents, forming distinctive domains that can be differentiated in terms of their characteristic length and time scales. These domains play vital role in physiological functions of the cell, such as acting as platforms for cell signalling [3], membrane trafficking [4], assembly of protein complexes [5], pathogen uptake [6, 7, 8], and vesicle trafficking [9]. Domain formation in plasma membrane has also been coupled to conformational changes such as domain budding [10]. Most of these cellular functions have been attributed to a special kind of lipid domains known as "rafts", which are usually perceived as dynamic nano-scale domains, rich in sterol and sphingolipids [11, 1, 12, 2]. However, their existence and size is still debated [13, 14, 15, 16, 17].

Based on the experimental phase diagram of dipalmitoyl phosphatidylcholine (DPPC) and Cholesterol mixture, proposed by Vist and Davis [18], J. H. Ipsen et al. were the first to theoretically characterize the lateral heterogeneities in this multicomponent lipid system [19]. They proposed the coexistence of two de-mixed liquid phases, categorized as "liquid ordered" (L_o) and "liquid disordered" (L_d). Later, based on a theoretical framework, M. Nielsen et al. ascribed the molecular origins of this de-mixing to the "decoupling nature" of cholesterol [20]. The L_o phase is characterized by high conformational order (similar to the gel phase (L_β)) and translational disorder (similar to nematic phase in liquid crystals (L_α)), usually comprising of saturated lipids. Absence of the long range intra-molecular conformational order is indicative of the L_d phase. Both these phases have been shown to possess similar translational diffusion of the order of $3\mu m^2/s$ [21].

Beyond multi-component model lipid systems [22, 23], L_o and L_d phases have also been observed in naturally occurring membranes [24, 25, 26]. Theoretical studies have tried to analyze the physical aspects of such phase separation towards understanding the underlying thermodynamics [27, 28, 29]. These lateral segregations are generally observed in lipid systems containing two different lipid types with well separated melting temperatures T_m, and cholesterol. Lipids with low T_m comprises of unsaturated lipids with a floppy conformation, and thus are found predominantly in the L_d phase. The lateral heterogeneities can be broadly classified into nano- and micro-domains, having dimensions ranging from 10-200 nm to a few microns, in model systems. A complete phase separation of the L_o and L_d phases corresponds to the thermodynamic equilibrium of the lipid system. However, the complex non-equilibrium processes occurring in the *in-vivo* cell membrane result in the stabilization of nano-domains over the thermodynamically more favourable micro-domains. Specific lipid composition of the cell membrane close to the critical points [30], role of linactant species [31, 32], intrinsic curvature of constituent lipids generating elastic energy [33], dynamical coupling to the actomyosin cytoskeleton [34, 35, 36, 37], and

conformational changes of membrane channel proteins [38] are a few example of such processes. In this work we study the effect of linactants in the stabilization of nano-domains in model systems, which represent "rafts" in real plasma membranes.

Linactants are hybrid lipids with one fully saturated and another unsaturated tail. The resulting molecular structure enables them to increase their compatibility with the two separate phases. These molecules stabilize the nano-domains by reducing line tension in structures (domains) that have a thermodynamically unfavourable high perimeter to area ratio. Line tension is the 2-dimensional analogue of surface tension, present at the interface of two phases, which arises due to the "hydrophobic mismatch" in the thickness of the L_o and L_d phases and membrane curvature [39, 40]. It is defined as the excess energy per unit length of a contact line where two or more distinct phases coexists. Owing to their "line active" nature, linactant molecules preferentially segregate at the interface of the two phases [41], thus lowering the unfavourable interaction energy and thereby, line tension. Line tension is one of the most important determinants of the existence, size, and segregation dynamics of domains in membrane systems [42, 43, 44]. They are known to favour small fluctuating domains and increase their lifetimes [45]. In the present study we have used PAPC as a model linactant molecule, with one tail similar to that of DPPC lipid and the other to that of DAPC lipid.

Our current study is focused on understanding the molecular origin of functionally important phase separation in model lipid systems. Toward this, we employ a characterization method which, while relatively new to biological literature, have been extensively used in the field of amorphous systems. Though seemingly distinct, amorphous materials or glasses have been shown to share striking similarities with bio-molecular systems. With functional proteins, they share some fundamental characteristics, in terms of their interior packing [**?**], rugged free energy surface [**?**], and relaxation mechanism [**?**]. Similar to lipid systems, super cooled glasses have also been found to show dynamic heterogeneity [**?**, **?**]. Motivated by such essential similarities between biological systems and amorphous granular materials, we borrow the idea of non-affine strain measurements, which was used by Falk and Langer in their seminal work [46] to identify the locations of irreversible plastic rearrangements in order to understand the phenomena of viscoplasticity in amorphous solids. In our work, we use this prescription to numerically calculate the degree of non-affineness in topological rearrangement of lipids in their local neighbourhood to distinguish between the L_o and L_d phases. It should be noted that affine and non-affine deformations have previously been employed on biological systems, in the area of cell mechanics to model actin cytoskeletal networks [47, 48, 49], but in a very different context. To the best of our knowledge, this is the first time that the degree of non-affineness, in the context of topological rearrangements [50, 51, 52], has been used to distinguish between the coexisting liquid phases in lipid systems.

Our main results are the following. We show that the degree of non-affineness, of the coexisting phases, is not biased by the chemical identity of the lipid species and serves as a useful tool to distinguish between

L_o and L_d phases, and identify the corresponding phase boundary. Using distance based clustering analysis, we show that cholesterol does not preferentially segregate with one of the lipid phase, and rather stations itself at the interface of the two phases. Finally, we also show that the effect of linactant on the liquid phase coexistence can be captured by the spread in the degree of non-affineness of the two separate phases.

The rest of the paper is organized as follows. In Section 2, we discuss our main results. Section 3 details the simulation and characterization methodologies. We conclude in Section 4 with a short summary and possible future directions.

2 Results and Discussion

In this section, we present the important results from current study. We begin with an exploration of the proposed numerical method in the context of the existing characterization techniques of L_o and L_d phases in the simulation literature, and then discuss its advantages. Next, the partitioning of cholesterol in such a phase separated lipid systems is investigated in terms of their clustering with the lipid domains. Finally, the effect of linactant molecules on phase boundaries is analyzed in terms of the spread in the degree of non-affineness of the two sub-phases.

2.1 Use of non-affine strain measurements to identify L_o and L_d phases:

There exist several experimental techniques to identify the two coexisting liquid phases in a lipid system. The most widely used methods involve the measurement of difference in bilayer thickness using AFM [53, 21] and SANS [44], conformational order of the alkyl chain using NMR tail order parameter [54, 55], and diffusion coefficients using FRET [**?**] and NMR [56]. These methods, along with the calculation of pair correlation functions, have been traditionally used to study the L_o and L_d phases in lipid systems simulations. To highlight the significance of our proposed method, involving non-affine strain measurements, we have discussed the results obtained from these existing methods in SI (Figure 1,2 and 3).

The difference in thickness of the lipid bilayer in the L_o and L_d phases has been termed as "hydrophobic mismatch". The chemical nature of the lipid species in the two phases leads to an inherent difference in their tail lengths. At the interface, the unfavourable exposure of hydrophobic part of the lipid of the thicker region generates excess boundary energy that manifests itself as line tension. As seen from (SI Figure S-1). The intermediate thickness values can be directly mapped to the lipids at the interface of L_o and L_d phases. Calculation of tail order parameter (S_{CD} or S_{CC})or the nematic order parameter requires the knowledge of position of the tail atoms in each lipid. Though S_{CD} and S_{CC} can demarcate the L_o and L_d regions (SI Figure S-2), this calculation is computationally expensive in comparison to

the method proposed in this work (as discussed in section 3.2). The inter and intra pair distribution functions of lipids in the L_o and L_d regions clearly show that these lipids prefer demixing (SI Figure S-3). The diffusion constant measured shown in Table 1 of SI shows that both the phases possess motion of comparable scale and have same order of magnitude. Hence though the exsisting techniques have been shown to distinguish the L_o and L_d regions in a de-mixed lipid system, we cannot single out a single technique that can indentify the L_o and L_d phases, be used to monitor kinetics of phase separation and capture the effect of linactant molecules all at ones. In this work we show that the method proposed is capable to preform all of the above.

In this work, we characterize the ordered/disordered regions in the lipid systems in terms of the distinction in their topological rearrangements. We quantify this difference by means of the degree of non-affineness associated with individual lipids within a neighbourhood of radius Ω. Taking a particular simulation snapshot as reference, we calculate the residual non-affineness (χ^2) for each lipid in the system at a later time of 10-100 ns. The phosphate head-group of the lipids denote the position of the lipids for the calculations and the neighbourhood radius Ω is taken to be 14 Å. The systems AA and CG systems on which the method was tested is given in Table 1 and Table 2. As shown in Figure S-4 in the SI, the value χ^2 increases monotonically, as the time window (Δt) between the two snapshots increases. The average values of χ^2, calculated over the equilibrium trajectories for the DAPC/DPPC/CHOL and DUPC/DPPC/CHOL CG systems using a time window Δt of ns, are shown in Figure 1. As evident from the figure, χ^2 values show higher dispersion for the later system. This can be attributed to the smaller sizes of domains in DUPC/DPPC/CHOL system, which are formed because of the lower degree of unsaturation of alkyl chain of DUPC, as compared to DAPC. DAPC/DPPC/CHOL forms continuous domains which is reflected in the lesser dispersion of χ^2 values, and also in the RDFs in SI Figure 3. The spread in χ^2 values can also give a qualitative information about the correlation decay length ξ, which is a measure of the size of fluctuations of the lipid domains [57, 58]. Higher values of ξ, indicative of larger wavelength fluctuations, can be associated with a high dispersion in χ^2 values. It should be emphasized that the calculation of χ^2 is computationally much less intensive in comparison to the estimation of ξ from the decay of spatial correlation function. As compared in Figure S-2, the dispersion in χ^2 values is much smaller than that in S_{CC} and carries important information on the very nature of the lipids.

Recently Hidden Markov Model (HMM) was used to identify L_o and L_d phases in all atom (AA) simulation of DOPC/DPPC/CHOL system [59]. To benchmark our analysis, we identify the liquid phases in the same AA systems using χ^2 values. To be consistent with earlier results, the mid-carbon sites of each of the lipid tails are used as evolving coordinates for the χ^2 analysis. Figure 2 shows a heat map of the lipid co-ordinates in the AA system, with χ^2 values as the colorbar. The ordered L_o nano-domain can be identified as a patch with the lowest χ^2 values and is mostly composed of DPPC

lipids, in agreement with the previous HMM analysis (Movie 1 SI). The disordered L_d phase is associated with comparatively higher χ^2 values. It should be stressed here, that the χ^2 analysis does not require the information on chemical identity of the lipids/cholesterol and is purely based on the topological data. Such a formulation allows it to capture the ordered/disordered micro-domains in CG and nano-domains in AA simulation trajectories. In Figure S-5 of SI, we show the profile of χ^2 values calculated on various AA systems with typical compositions leading to pure L_o, pure L_d, and mixed L_o/L_d phases. The pure L_o phase is identified with much lower χ^2 values as compared to pure L_d phase, while the mixed phases show a clear combination of low and high values indicating a bimodal distribution.

Beyond the ability to discern between ordered/disordered domains, χ^2 values can also be used to monitor the kinetics of domain formation. The initial stage of phase separation has been proposed to occur though spinodal decomposition near the critical point and via nucleation otherwise [60]. Figure 3 shows the long tail distribution of χ^2 values for DAPC and DPPC lipids in atomistic DAPC/DPPC/CHOL system as the simulation advances. For this part of the calculations, the values of χ^2 have been segregated based on the lipid kind and the distributions are calculated separately. The overlapping region in the distribution corresponds to the lipids that do not belong to a pure L_o or L_d phase. As apparent from the figure, the overlap in the distribution decreases with time indicating separation of the two phases, and thus can be used as a measure to study the segregation dynamics. As shown in Figure 4 as the area of the overalping region converges the system is said to have attained equilibrium. The trend in the overlap of long tail distribution of the χ^2 values can be an indicative of a nucleation process.

2.2 Identifying the "true" interface of ordered/disordered regions:

Unlike most of the traditionally used techniques, measurement of residual non-affineness does not require *a priori* knowledge on chemical identity of the lipids to distinguish between L_o and L_d phases. Traditional way of identification of the boundary lipids involves the association of saturated and unsaturated lipids to different phases (Carla M Rosetti et al., 2017, JPCb). The heat map in Figure 5 for AA DOPC/DPPC/CHOL system shows that not all DPPC lipids form the L_o phase as previously assumed in HMM calculations [59], rather some DOPC and cholesterol sites also belong this L_o phase. Our calculations, thus, show that "orderness" is environment dependent and need not be associated with the chemical identity of the lipids. As seen in Figure 2, some of the DPPC lipids have higher χ^2 and these can be rightly identified as those belonging to the L_d phase. Lower S_{CD} of these DPPC lipids with higher χ^2 values also shows that they are less ordered. In Figure 5, shown are the contoured heat maps of the DAPC/DPPC/CHOL and DUPC/DPPC/CHOL systems, with averaged χ^2 values as the colorbar. As evident, the boundary lipids acquire intermediate χ^2 values, and thus can be used to detect lipids that form the interface of L_o and L_d phases. Further the fluctuation in this domain boundary shown in Figure S-6 can be used to quantify line tension in the system.

2.3 Cholesterol partitioning in L_o and L_d phases:

As discussed in the last section, the ordered phase in the membrane is not formed exclusively by the saturated lipids, but is also composed of some unsaturated lipids and cholesterol. Therefore, to study the behavior of cholesterol in the phase separated system of ordered and disordered lipids, we perform cluster analysis on the atomistic trajectory of DOPC/DPPC/CHOL system. The mid points of the two tails of each lipid are taken as the evolving coordinates. A distanced based clustering algorithm is used with cutoffs 5, 6, 7, and 8 Å. The variation in N_S, the occurrence probability (number of clusters with size S), with different cutoff distances for DPPC and DOPC lipids, is shown in Figure 6. For both the lipid types, we also calculate the cluster size distribution by taking the cholesterol sites into account. For a given cutoff distance, N_S, for both DOPC and DPPC lipids, increases when the cholesterols are included in the analysis. The occurrence probability of larger clusters ($S > 100$) increases noticeably for the two lipid types. Such a common trend of increase in N_S for both the lipids upon incorporating the cholesterol sites in the calculation, especially for large S, indicates the formation of large clusters of DOPC and DPPC lipids that also include cholesterols. This observation suggests that the cholesterol does not segregate preferentially with either of the lipid types, but rather is located at the interface of the DPPC/DOPC clusters. This is in line with the previous study [59], which proposed that the cholesterol does not disrupt the hexagonal packing of DPPC lipids and hence are stationed at the interface of DPPC and DOPC lipid domains. Same calculations were also performed on the other L_o/L_d phase separated systems (Figure S-7, S-8) which also show that cholestrol is present at the interface of lipids in the ordered and disordered phases.

2.4 Predicting the effect of linactant molecules on phase boundaries using χ^2 values:

Theoretical study shows that line tension depends quadratically on thickness difference between the L_o and L_d phases [61]. Linactant molecules lower the line tension across the boundary of the two phases by reducing the hydrophobic mismatch [62]. To study the effect of linactant molecules on the phase segregation in DAPC/DPPC/CHOL system, we compute the distribution of χ^2 values for both the lipid kinds with increasing linactant (PAPC) ratio (X: number of PAPC molecules to unsaturated lipids), which is shown in Figure 7. As discussed in earlier sections, the overlap in the long tail probability distribution indicates the lipids at the interface of L_o and L_d phases, and thus can be monitored as an indication of disruption of the phase boundary and thermal fluctuations. We find that the overlap in χ^2 distribution monotonically increases with increasing linactant ratio, suggesting the domain boundary fluctuations increase with increasing number of "interfacial" lipids. Eventually, beyond a certain concentration of these line active molecules, the phase segregation is almost lost as the saturated and unsaturated lipids

start to mix without an energy penalty.

Figure 7 also indicates the L_d phase to be more affected by the linactant molecules, than the L_o phase. The dispersion of χ^2 values, in the L_d phase, increases with increase in linactant ratio, as indicated by the lowering of the peak and subsequent flattening. This inference is similar to the analysis performed by Carla et al. [62] on the same lipid system. They show that the affinity of the saturated tail of PAPC towards the L_o region decreases with increase in PAPC ratio, thus having more effect on the unsaturated DAPC lipids. We calculate the probability distributions of tail order parameter (S_{CC}) of DAPC and DPPC lipids, for all the linactant ratios probed in their study, which is shown in Figure 10. While the S_{CC} distributions of DPPC lipids do not change significantly with linactant ratio, those of DAPC lipids change remarkably from a single peak to a wider distribution. The average order parameter values for DPPC changes from 0.611 to 0.554, and that for DAPC from 0.094 to 0.053 for X=0.1 to 0.5. Linactants act by first increasing the disorderedness of DAPC lipids upto a critical concentration of X=0.36 and then ordering them. This trend is also seen in Figure 10. After X=0.36, a finite fraction of the ordered lipids become floppy while some of the disordered lipids become linear, as can be inferred from the spread in the corresponding distributions. Such a redistribution leads to a decrease in the thickness mismatch between the two lipid domains, thereby decreasing the line tension.

3 Materials and Methods

In this section we summarize the details of the models, simulation methodologies, and numerical implementation. We start by highlighting the details of AA and CG simulations in the first subsection. We then discuss various characterization methods used in this work, including the mathematical construct, we followed, to calculate χ^2.

3.1 Model and Simulation details

3.1.1 All Atom Simulations

A diffusion constant of the order of $10^{-7} cm^2/s$ for lipids in all atom representation requires the systems to be evolved for several microseconds in order to achieve equilibrium lateral distribution. Therefore, such simulations are computationally expensive. The all atom simulation trajectories used in this work were borrowed from Edward Lyman's group in Delaware. The trajectories constituted six ternary lipid bilayer simulations performed on Anton supercomputer. Position and velocities were collected at an interval of 240 ps. The relevant details of the all atom systems are summarized in Table 2. Further technical details of the simulation set up can be found in the corresponding references [63, 59].

All Atom Systems					
Lipid system	Composition	Phase	Temperature (K)	System size (nm)	Duration (μs)
PSM/DOPC/CHOL	0.15/0.82/0.03	Ld	295	13.42×13.42	0.81
PSM/DOPC/CHOL	0.64/0.03/0.33	Lo	295	10.63×10.63	0.95
PSM/DOPC/CHOL	0.43/0.38/0.19	Lo/Ld	295	10.86×10.86	4.54
PSM/POPC/CHOL	0.61/0.08/0.31	Lo	295	10.62×10.62	9.08
PSM/POPC/CHOL	0.47/0.32/0.21	Lo/Ld	295	10.87×10.87	6.88
DPPC/DOPC/CHOL	0.37/0.36/0.27	Lo/Ld	298	9.53×9.53	9.43

Table 1: Simulation details of various all atom trajectories analyzed in this work.

3.1.2 Coarse Grained (CG) simulations

CG simulation on 35%/35%/30% DAPC/DPPC/CHOL ternary lipid system, of size $\sim 25 \times 25$ Å^2, was set up using CHARMM-GUI Martini membrane builder web server [64, 65]. The tensionless membrane was simulated using GROMACS 5.0.2 [66] in NPT ensemble at 295 K temperature and 1 bar pressure. A constant temperature was maintained using velocity rescaling and a constant pressure using Parrinelo-Rahman barostat [67] with relaxation times of 1.0 ps and 2.0 ps respectively. Cut-off and shift distances of 1.2 nm and 0.9 nm to 1.2 nm respectively were used for van der Waals interactions. To simulate a tensionless bilayer, semi-isotropic pressure coupling was performed independently in the lateral and normal directions with a compressibility constant of 3×10^{-4} bar^{-1}. The restraints, initially applied on the lipid head-groups in order to maintain the bilayer structure, were gradually released in the equilibration phase. The multi-component bilayer system was then evolved for 1.6 μs and positions and velocities were collected at a frequency of 40 ns, until equilibrium phase separation was achieved.

The CG trajectory for martini coarse-grained DUPC/DPPC/CHOL lipid mixture was obtained from Peter Tieleman's group at Calgary [68]. The system was evolved for 11 μs and positions and velocities were collected at every 10 ns. Trajectories for systems with different linactant fractions were borrowed from Carla M. Rosetti's lab at Argentina [62]. Positions and velocities of these systems were written at a frequency of 60 ns. Details of all the three CG systems are summarized in Table 3 and 4.

Coarse grain systems				
Lipid system	Composition	Phase	Temperature(K)	System size(nm)
DAPC/DPPC/CHOL	0.35/0.35/0.30	Lo/Ld	295	24.82×24.82
DUPC/DPPC/CHOL	0.25/0.42/0.33	Lo/Ld	290	35.5×35.5

Table 2: Simulation details of the CG systems (Martini).

3.2 Numerical Implementation

We calculate the degree of non-affineness, associated with any lipid in an evolving membrane system, based on the topological rearrangements occurring in a local neighborhood around it [46]. An affine deformation is always associated with a uniform strain. For non-affine case, the total deformation can be broken down to an affine and a residual part. Thus, the degree of non-affineness (χ^2) measures the

Effect of linactant	
Hybrid lipid	$x = \frac{Hybrid}{Hybrid+Symmetric}$
PAPC	0
PAPC	0.1
PAPC	0.18
PAPC	0.36
PAPC	0.5

Table 3: Simulation details of various CG ternary lipid systems with linactant (Martini).

residual non-affine content of a deformation. Following the mathematical construct of Falk and Langer [46], the residual deviation from affine deformation during a time interval $[t, t + \Delta t]$ is given by

$$\chi^2_\Omega(t, \Delta t) = \sum_{n=1}^{N} \sum_{i=1}^{d} \left(r^i_n(t + \Delta t) - r^i_0(t + \Delta t) - \sum_{j=1}^{d} (\delta_{ij} + \epsilon_{ij}) \times \left[r^j_n(t) - r^j_0(t) \right] \right)^2, \tag{1}$$

where the indices i and j run through the spatial coordinates for dimension d and n runs over the N lipids in the neighbourhood Ω, defined within a cutoff distance around the reference lipid $n = 0$. δ_{ij} is the Kroneker delta function. ϵ_{ij} is the strain associated with the maximum possible affine part of the deformation and thus, minimizes $\chi^2_\Omega(t, \Delta t)$. ϵ_{ij} and $\chi^2_\Omega(t, \Delta t)$ can be calculated easily following the prescription given in the original reference.

For all the calculations the head-group sites were used to as reference to represent a lipid. In order to compare results from AJ Scodt et al. [59], the mid tail sites were used in the case of DOPC/DPPC/CHOL AA system. The calculations on AA systems were performed with $\Delta t = 240\, ps$. For DUPC/DPPC/CHOL CG systems, $\Delta t = 100\ ns$ in CG timescales and $\Delta t = 4\ ns$ for DAPC/DPPC/CHOL CG systems. For DAPC/DPPC/CHOL systems with varying linactant concentrations $\Delta t = 60\ ns$ was used.

In addition to the degree of non-affineness calculation, analyses traditionally used in the simulation literature on lipid systems to distinguish between L_o and L_d phases, including the calculation of radial distribution functions, tail order parameter, diffusion co-efficient from mean square displacement, thickness and area per lipid, were carried out. The ability of these measurements in characterizing the L_o and L_d phases was investigated and compared to that of non-affineness calculation.

4 Summary and Conclusion

In this work, we explore the feasibility of utilizing the information on topological rearrangement of lipids, to characterize the phase separation in a model membrane system. We numerically calculate the degree of non-affineness (χ^2), associated with evolving lipids in their local neighbourhood, to distinguish between the liquid ordered and liquid disordered phases.

Apart from identifying these phases, χ^2 values can also be used to monitor the kinetics of domain

segregation. Such a kinetic study can distinguish between the two types of phase separation: nucleation and growth, and spinodal decomposition, depending on the nature of domain evolution. The non-affine parameter contains information about the local neighbourhood of the lipids and hence can be used to identify lipids at the boundary of the two phases. Unlike the existing methods that are traditionally used in simulation studies and experiments, the boundary thus traced out is not biased by chemical identity of the lipids and so identifies the "true interface". The effect of linactant molecules that preferentially segregate at the interface of L_o and L_d regions can be captured using the overlap between the probability distribution of χ^2 values for lipids in both phases. We show that linactant molecules lower the line tension by decreasing hydrophobic mismatch between the lipids that form the interface of the two phases.

On the methodology front, we propose a computationally less expensive method of characterizing L_o and L_d phases in atomistic and coarse-grained simulation studies of bio-membranes. This method can also be utilized in kinetics experiments, where images separated by timescales as large at 0.5 μs can be analyzed without performing complicated image processing. While identification of individual lipids in experiments can be severely limited by the experimental resolution, one can nonetheless utilize this method in the study of kinetics of large-scale membrane features such as lipid rafts and protein assembly, and tissues.

5 Acknoledgement

The authors thank Edward Lyman, Peter Tieleman, and Carla M. Rosetti's lab for sharing the simulation trajectories. The financial support from Indian Institute of Science-Bangalore and the HPC facility "Arjun", setup from grants by Department of Biotechnology (DBT-India), are greatly acknowledged.

References

[1] Kai Simons and Elina Ikonen. Functional rafts in cell membranes. *Nature*, 387(6633):569, 1997.

[2] DA Brown and E London. Functions of lipid rafts in biological membranes. *Annual review of cell and developmental biology*, 14(1):111–136, 1998.

[3] Katharina Gaus, Elena Chklovskaia, Barbara Fazekas de St Groth, Wendy Jessup, and Thomas Harder. Condensation of the plasma membrane at the site of t lymphocyte activation. *J Cell Biol*, 171(1):121–131, 2005.

[4] Gerrit van Meer, EH Stelzer, Roel W Wijnaendts-van Resandt, and Kai Simons. Sorting of sphingolipids in epithelial (madin-darby canine kidney) cells. *The Journal of cell biology*, 105(4):1623–1635, 1987.

[5] Katharina Gaus, Soazig Le Lay, Nagaraj Balasubramanian, and Martin A Schwartz. Integrin-mediated adhesion regulates membrane order. *The Journal of cell biology*, 174(5):725–734, 2006.

[6] Frank Lafont and F Gisou Van Der Goot. Bacterial invasion via lipid rafts. *Cellular microbiology*, 7(5):613–620, 2005.

[7] Sung-Tae Yang, Volker Kiessling, James A Simmons, Judith M White, and Lukas K Tamm. Hiv gp41-mediated membrane fusion occurs at edges of cholesterol-rich lipid domains. *Nature chemical biology*, 11(6):424–431, 2015.

[8] Sung-Tae Yang, Volker Kiessling, and Lukas K Tamm. Line tension at lipid phase boundaries as driving force for hiv fusion peptide-mediated fusion. *Nature communications*, 7:11401, 2016.

[9] Christine Salaün, Declan J James, and Luke H Chamberlain. Lipid rafts and the regulation of exocytosis. *Traffic*, 5(4):255–264, 2004.

[10] Dzung H Nguyen and James EK Hildreth. Evidence for budding of human immunodeficiency virus type 1 selectively from glycolipid-enriched membrane lipid rafts. *Journal of virology*, 74(7):3264–3272, 2000.

[11] Richard GW Anderson and Ken Jacobson. A role for lipid shells in targeting proteins to caveolae, rafts, and other lipid domains. *Science*, 296(5574):1821–1825, 2002.

[12] Kai Simons and Winchil LC Vaz. Model systems, lipid rafts, and cell membranes. *Annu. Rev. Biophys. Biomol. Struct.*, 33:269–295, 2004.

[13] A Pralle, P Keller, E-L Florin, Kai Simons, and JK Heinrich Hörber. Sphingolipid–cholesterol rafts diffuse as small entities in the plasma membrane of mammalian cells. *The Journal of cell biology*, 148(5):997–1008, 2000.

[14] Pranav Sharma, Rajat Varma, RC Sarasij, Karine Gousset, G Krishnamoorthy, Madan Rao, Satyajit Mayor, et al. Nanoscale organization of multiple gpi-anchored proteins in living cell membranes. *Cell*, 116(4):577–589, 2004.

[15] Kripa Gowrishankar, Subhasri Ghosh, Suvrajit Saha, C Rumamol, Satyajit Mayor, and Madan Rao. Active remodeling of cortical actin regulates spatiotemporal organization of cell surface molecules. *Cell*, 149(6):1353–1367, 2012.

[16] Ian A Prior, Cornelia Muncke, Robert G Parton, and John F Hancock. Direct visualization of ras proteins in spatially distinct cell surface microdomains. *The Journal of cell biology*, 160(2):165–170, 2003.

[17] Dylan M Owen, Astrid Magenau, David Williamson, and Katharina Gaus. The lipid raft hypothesis revisited–new insights on raft composition and function from super-resolution fluorescence microscopy. *Bioessays*, 34(9):739–747, 2012.

[18] Margus R Vist and James H Davis. Phase equilibria of cholesterol/dipalmitoylphosphatidylcholine mixtures: deuterium nuclear magnetic resonance and differential scanning calorimetry. *Biochemistry*, 29(2):451–464, 1990.

[19] J Hjort Ipsen, G Karlström, OG Mourtisen, H Wennerström, and MJ Zuckermann. Phase equilibria in the phosphatidylcholine-cholesterol system. *Biochimica et Biophysica Acta (BBA)-Biomembranes*, 905(1):162–172, 1987.

[20] Morten Nielsen, Ling Miao, John H Ipsen, Martin J Zuckermann, and Ole G Mouritsen. Off-lattice model for the phase behavior of lipid-cholesterol bilayers. *Physical Review E*, 59(5):5790, 1999.

[21] Marie-Cécile Giocondi, Daisuke Yamamoto, Eric Lesniewska, Pierre-Emmanuel Milhiet, Toshio Ando, and Christian Le Grimellec. Surface topography of membrane domains. *Biochimica et Biophysica Acta (BBA)-Biomembranes*, 1798(4):703–718, 2010.

[22] G Pabst, N Kučerka, M-P Nieh, MC Rheinstädter, and J Katsaras. Applications of neutron and x-ray scattering to the study of biologically relevant model membranes. *Chemistry and Physics of Lipids*, 163(6):460–479, 2010.

[23] Michal Belička, Anna Weitzer, and Georg Pabst. High-resolution structure of coexisting nanoscopic and microscopic lipid domains. *Soft Matter*, 13(9):1823–1833, 2017.

[24] C Dietrich, LA Bagatolli, ZNa Volovyk, NL Thompson, M Levi, K Jacobson, and E Gratton. Lipid rafts reconstituted in model membranes. *Biophysical journal*, 80(3):1417–1428, 2001.

[25] Jorge Bernardino de la Serna, Jesus Perez-Gil, Adam C Simonsen, and Luis A Bagatolli. Cholesterol rules direct observation of the coexistence of two fluid phases in native pulmonary surfactant membranes at physiological temperatures. *Journal of Biological Chemistry*, 279(39):40715–40722, 2004.

[26] Hideaki Mizuno, Mitsuhiro Abe, Peter Dedecker, Asami Makino, Susana Rocha, Yoshiko Ohno-Iwashita, Johan Hofkens, Toshihide Kobayashi, and Atsushi Miyawaki. Fluorescent probes for superresolution imaging of lipid domains on the plasma membrane. *Chemical Science*, 2(8):1548–1553, 2011.

[27] Jean Wolff, Carlos M Marques, and Fabrice Thalmann. Thermodynamic approach to phase coexistence in ternary phospholipid-cholesterol mixtures. *Physical review letters*, 106(12):128104, 2011.

[28] Shigeyuki Komura and David Andelman. Physical aspects of heterogeneities in multi-component lipid membranes. *Advances in colloid and interface science*, 208:34–46, 2014.

[29] G Garbes Putzel and Michael Schick. Phenomenological model and phase behavior of saturated and unsaturated lipids and cholesterol. *Biophysical journal*, 95(10):4756–4762, 2008.

[30] Sarah L Veatch, Olivier Soubias, Sarah L Keller, and Klaus Gawrisch. Critical fluctuations in domain-forming lipid mixtures. *Proceedings of the National Academy of Sciences*, 104(45):17650–17655, 2007.

[31] Robert Brewster, Philip A Pincus, and Samuel A Safran. Hybrid lipids as a biological surface-active component. *Biophysical journal*, 97(4):1087–1094, 2009.

[32] VAJ Frolov, Yu A Chizmadzhev, FS Cohen, and J Zimmerberg. "entropic traps" in the kinetics of phase separation in multicomponent membranes stabilize nanodomains. *Biophysical journal*, 91(1):189–205, 2006.

[33] Reinhard Lipowsky. Budding of membranes induced by intramembrane domains. *Journal de Physique II*, 2(10):1825–1840, 1992.

[34] Jordi Gómez-Llobregat, Javier Buceta, and Ramon Reigada. Interplay of cytoskeletal activity and lipid phase stability in dynamic protein recruitment and clustering. *Scientific reports*, 3, 2013.

[35] Arun Yethiraj and James C Weisshaar. Why are lipid rafts not observed in vivo? *Biophysical journal*, 93(9):3113–3119, 2007.

[36] Md Kabir Uddin Sikder, Kyle A Stone, PB Sunil Kumar, and Mohamed Laradji. Combined effect of cortical cytoskeleton and transmembrane proteins on domain formation in biomembranes. *The Journal of chemical physics*, 141(5):08B603_1, 2014.

[37] Alf Honigmann, Sina Sadeghi, Jan Keller, Stefan W Hell, Christian Eggeling, and Richard Vink. A lipid bound actin meshwork organizes liquid phase separation in model membranes. *Elife*, 3:e01671, 2014.

[38] H Aranda-Espinoza, A Berman, N Dan, P Pincus, and S Safran. Interaction between inclusions embedded in membranes. *Biophysical journal*, 71(2):648–656, 1996.

[39] Dominic J Benvegnu and Harden M McConnell. Line tension between liquid domains in lipid monolayers. *The Journal of Physical Chemistry*, 96(16):6820–6824, 1992.

[40] Harden M McConnell. Structures and transitions in lipid monolayers at the air-water interface. *Annual Review of Physical Chemistry*, 42(1):171–195, 1991.

[41] Robert Brewster and Samuel A Safran. Line active hybrid lipids determine domain size in phase separation of saturated and unsaturated lipids. *Biophysical journal*, 98(6):L21–L23, 2010.

[42] Aurelia R Honerkamp-Smith, Pietro Cicuta, Marcus D Collins, Sarah L Veatch, Marcel den Nijs, M Schick, and Sarah L Keller. Line tensions, correlation lengths, and critical exponents in lipid membranes near critical points. *Biophysical journal*, 95(1):236–246, 2008.

[43] Ana J García-Sáez, Salvatore Chiantia, and Petra Schwille. Effect of line tension on the lateral organization of lipid membranes. *Journal of Biological Chemistry*, 282(46):33537–33544, 2007.

[44] Frederick A Heberle, Robin S Petruzielo, Jianjun Pan, Paul Drazba, Norbert Kučerka, Robert F Standaert, Gerald W Feigenson, and John Katsaras. Bilayer thickness mismatch controls domain size in model membranes. *Journal of the American Chemical Society*, 135(18):6853–6859, 2013.

[45] Benoit Palmieri, Tetsuya Yamamoto, Robert C Brewster, and Samuel A Safran. Line active molecules promote inhomogeneous structures in membranes: Theory, simulations and experiments. *Advances in colloid and interface science*, 208:58–65, 2014.

[46] ML Falk and JS Langer. Dynamics of viscoplastic deformation in amorphous solids. *Physical Review E*, 57(6):7192, 1998.

[47] PR Onck, T Koeman, T Van Dillen, and Erik van der Giessen. Alternative explanation of stiffening in cross-linked semiflexible networks. *Physical review letters*, 95(17):178102, 2005.

[48] Mo Bai, Andrew R Missel, William S Klug, and Alex J Levine. The mechanics and affine–nonaffine transition in polydisperse semiflexible networks. *Soft Matter*, 7(3):907–914, 2011.

[49] Yifan Wang, Jinghai Gong, Denis Wirtz, and Benjamin W Schafer. Affine and non-affine deformations quantified in cytoskeletal networks through three-dimensional form-finding model. *Journal of the Mechanical Behavior of Biomedical Materials*, 72:52–65, 2017.

[50] Saswati Ganguly, Surajit Sengupta, Peter Sollich, and Madan Rao. Nonaffine displacements in crystalline solids in the harmonic limit. *Physical Review E*, 87(4):042801, 2013.

[51] A Zaccone, P Schall, and EM Terentjev. Microscopic origin of nonlinear nonaffine deformation in bulk metallic glasses. *Physical Review B*, 90(14):140203, 2014.

[52] Qi Wen, Anindita Basu, Paul A Janmey, and Arjun G Yodh. Non-affine deformations in polymer hydrogels. *Soft matter*, 8(31):8039–8049, 2012.

[53] Chunbo Yuan, Jennifer Furlong, Pierre Burgos, and Linda J Johnston. The size of lipid rafts: an atomic force microscopy study of ganglioside gm1 domains in sphingomyelin/dopc/cholesterol membranes. *Biophysical journal*, 82(5):2526–2535, 2002.

[54] Joachim Seelig and Werner Niederberger. Deuterium-labeled lipids as structural probes in liquid crystalline bilayers. deuterium magnetic resonance study. *Journal of the American Chemical Society*, 96(7):2069–2072, 1974.

[55] Harden McConnell and Arun Radhakrishnan. Theory of the deuterium nmr of sterol–phospholipid membranes. *Proceedings of the National Academy of Sciences*, 103(5):1184–1189, 2006.

[56] Andrey Filippov, Greger Orädd, and Göran Lindblom. The effect of cholesterol on the lateral diffusion of phospholipids in oriented bilayers. *Biophysical journal*, 84(5):3079–3086, 2003.

[57] Sarah L Veatch, Pietro Cicuta, Prabuddha Sengupta, Aurelia Honerkamp-Smith, David Holowka, and Barbara Baird. Critical fluctuations in plasma membrane vesicles. *ACS chemical biology*, 3(5):287–293, 2008.

[58] Aurelia R Honerkamp-Smith, Sarah L Veatch, and Sarah L Keller. An introduction to critical points for biophysicists; observations of compositional heterogeneity in lipid membranes. *Biochimica et Biophysica Acta (BBA)-Biomembranes*, 1788(1):53–63, 2009.

[59] Alexander J Sodt, Michael Logan Sandar, Klaus Gawrisch, Richard W Pastor, and Edward Lyman. The molecular structure of the liquid-ordered phase of lipid bilayers. *Journal of the American Chemical Society*, 136(2):725–732, 2014.

[60] Carla M Rosetti, Agustín Mangiarotti, and Natalia Wilke. Sizes of lipid domains: What do we know from artificial lipid membranes? what are the possible shared features with membrane rafts in cells? *Biochimica et Biophysica Acta (BBA)-Biomembranes*, 2017.

[61] Peter I Kuzmin, Sergey A Akimov, Yuri A Chizmadzhev, Joshua Zimmerberg, and Fredric S Cohen. Line tension and interaction energies of membrane rafts calculated from lipid splay and tilt. *Biophysical journal*, 88(2):1120–1133, 2005.

[62] Carla M Rosetti, Guillermo G Montich, and Claudio Pastorino. Molecular insight into the line tension of bilayer membranes containing hybrid polyunsaturated lipids. *The Journal of Physical Chemistry B*, 121(7):1587–1600, 2017.

[63] Alexander J Sodt, Richard W Pastor, and Edward Lyman. Hexagonal substructure and hydrogen bonding in liquid-ordered phases containing palmitoyl sphingomyelin. *Biophysical journal*, 109(5):948–955, 2015.

[64] Sunhwan Jo, Taehoon Kim, Vidyashankara G Iyer, and Wonpil Im. Charmm-gui: a web-based graphical user interface for charmm. *Journal of computational chemistry*, 29(11):1859–1865, 2008.

[65] Yifei Qi, Helgi I Ingólfsson, Xi Cheng, Jumin Lee, Siewert J Marrink, and Wonpil Im. Charmm-gui martini maker for coarse-grained simulations with the martini force field. *Journal of chemical theory and computation*, 11(9):4486–4494, 2015.

[66] Berk Hess, Carsten Kutzner, David Van Der Spoel, and Erik Lindahl. Gromacs 4: algorithms for highly efficient, load-balanced, and scalable molecular simulation. *Journal of chemical theory and computation*, 4(3):435–447, 2008.

[67] Michele Parrinello and Aneesur Rahman. Polymorphic transitions in single crystals: A new molecular dynamics method. *Journal of Applied physics*, 52(12):7182–7190, 1981.

[68] Svetlana Baoukina, Eduardo Mendez-Villuendas, WF Drew Bennett, and D Peter Tieleman. Computer simulations of the phase separation in model membranes. *Faraday discussions*, 161:63–75, 2013.

Figures

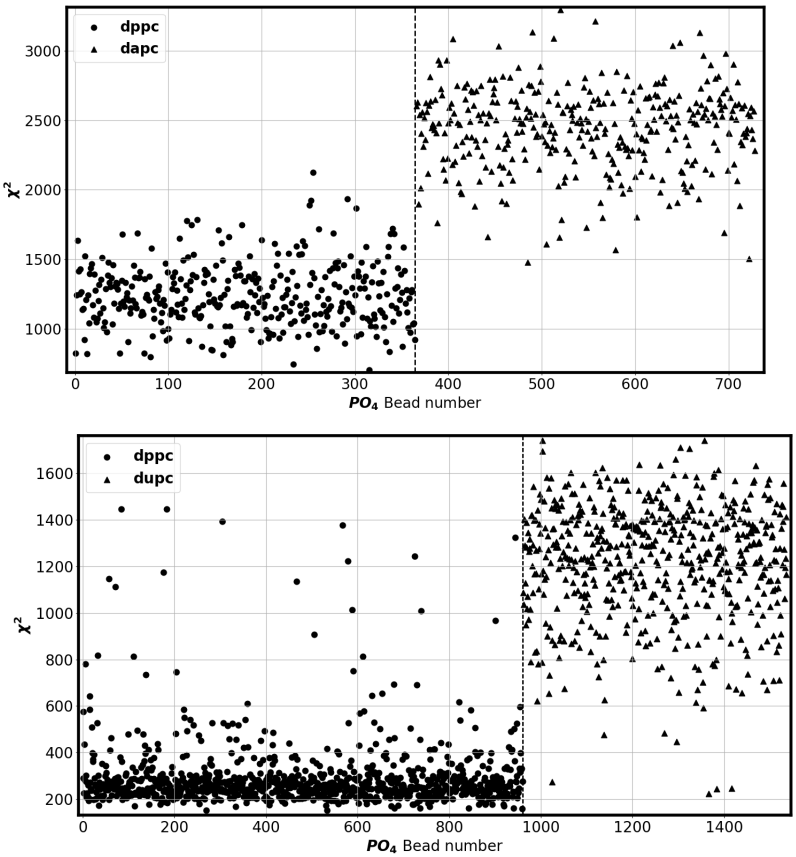

Figure 1: Bimodal distribution of χ^2 values calculated for the PO_4 groups for (top) DAPC/DPPC/CHOL system and (bottom) DUPC/DPPC/CHOL system. The higher dispersion in χ^2 values for the latter is indicative of presence of less continuous and more dispersed phase separated domain system. The difference between the relative χ^2 values for L_o and L_d lipids in both these cases is due to the time interval for which χ^2 is calculated of each of these systems. Figure (1) in SI shows that the difference in χ^2 values for these two phases increases linearly with time.

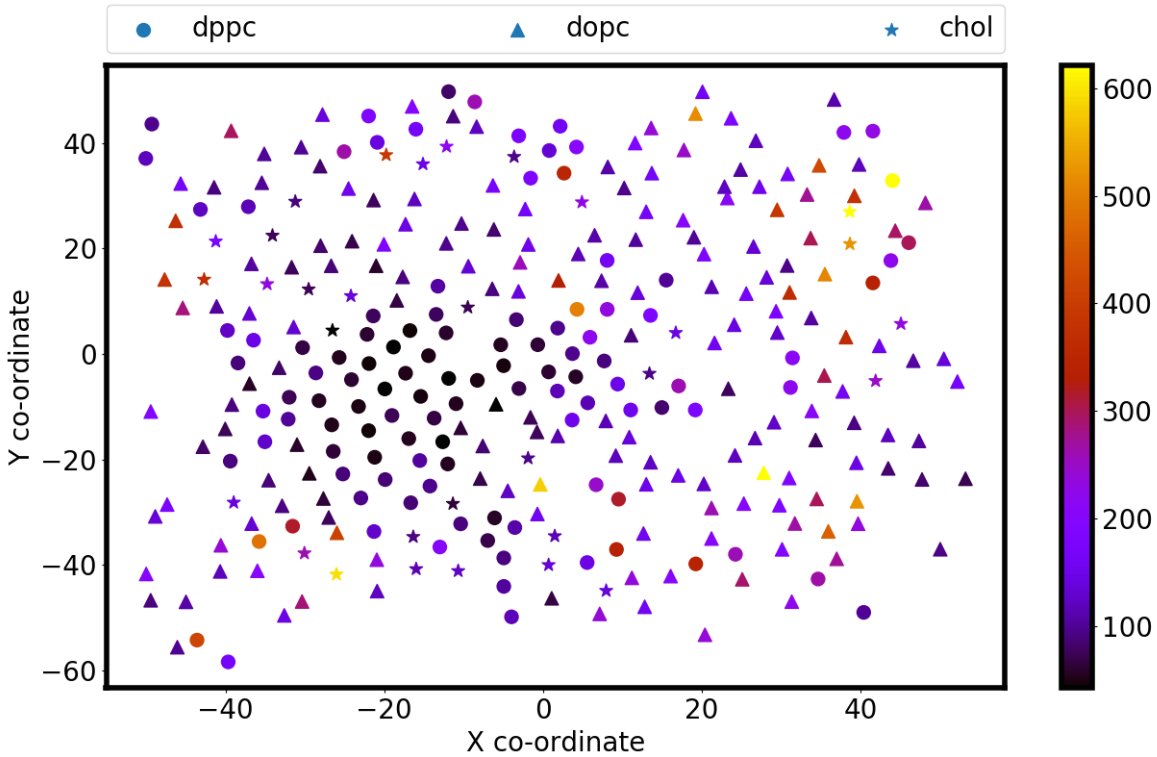

Figure 2: Position of DOPC, DPPC and CHOL mid atom sites color coded with the corresponding χ^2 values is show. DPPC lipid sites shown as circles for a nanodomain which is captured by the low χ^2 values. Other DPPC lipid sites that are not part of this continuous domain have higher chi^2 values. This indicated that χ^2 values can be used to identify L_o and L_d phases without being biased by chemical identify of the lipids.

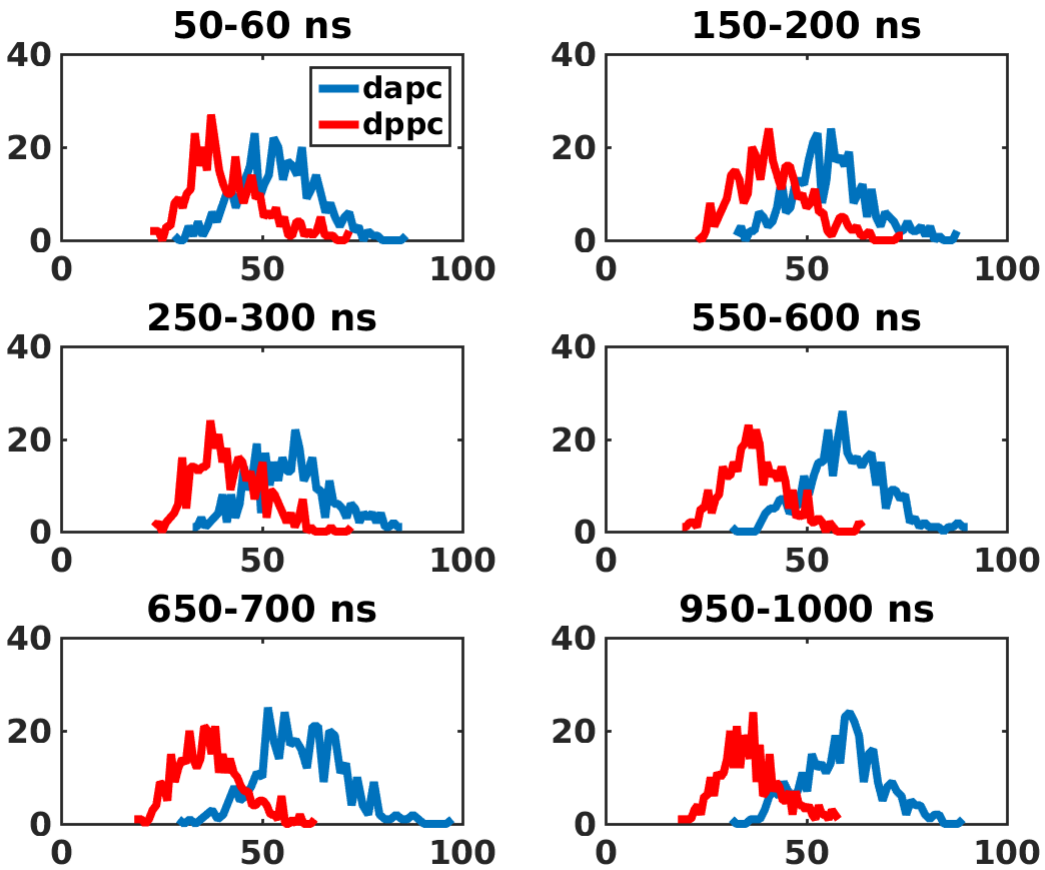

Figure 3: χ^2 values capturing dynamics of phase segregation in DAPC/DPPC/CHOL system. The degree of phase separation can be monitored as by the amount of overlap in the long tail distributions of χ^2 values for each lipid type. The bimodal probability distribution of χ^2 values becomes more apparent as the system evolves into being completely phase separated.

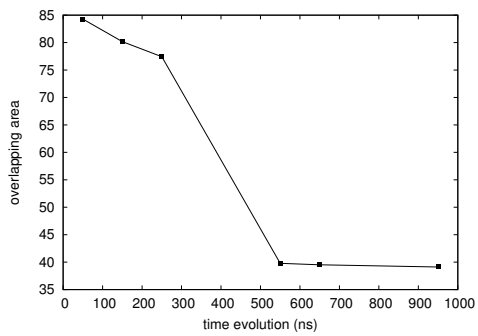

Figure 4: The evolution of area of the overlapping region of the long tails of χ^2 distributions can be used to monitor domain growth. As the area of the overlapping region reaches a given value asympotically, the system is said to have attained equilibrium.

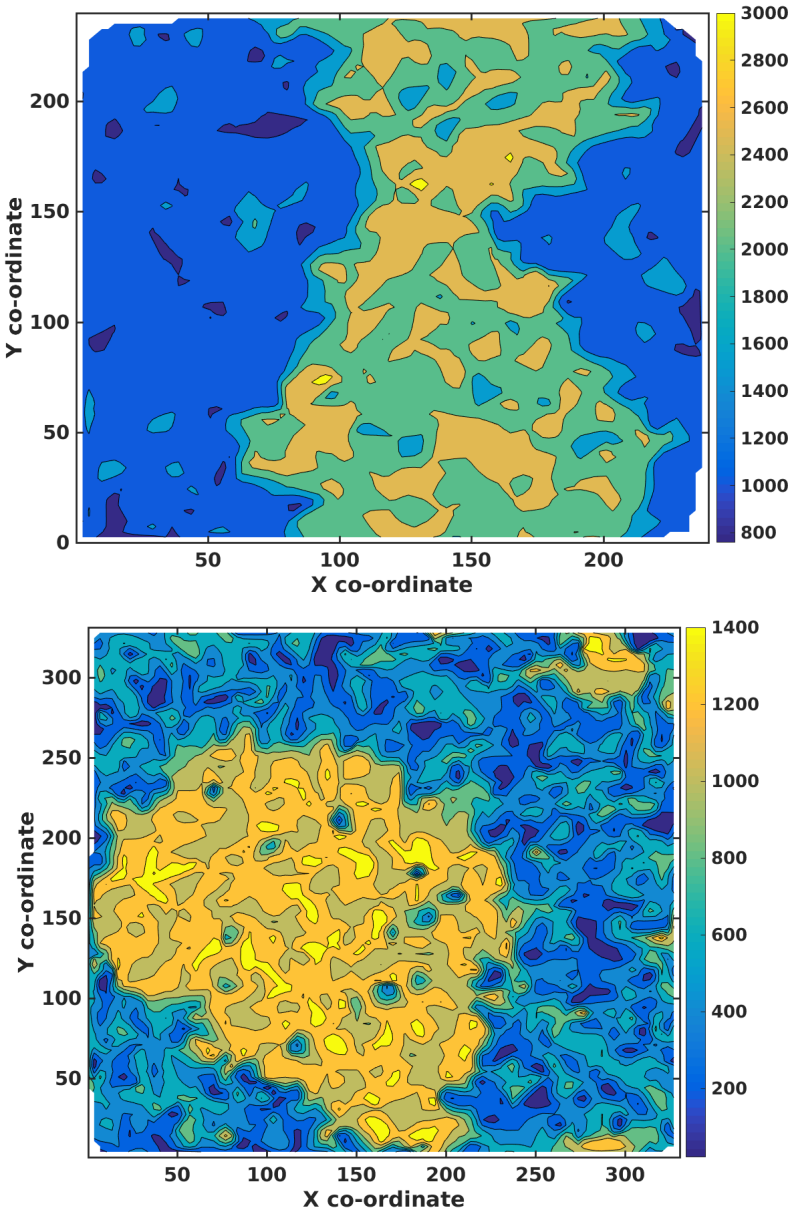

Figure 5: Contour map with χ^2 has the contour height shows for (top) DAPC/DPPC/CHOL system that lipids with χ^2 values between 45-55 and (bottom) for DUPC/DPPC/CHOL system lipids with χ^2 values between 700-900 can be identified as the boundary lipids.

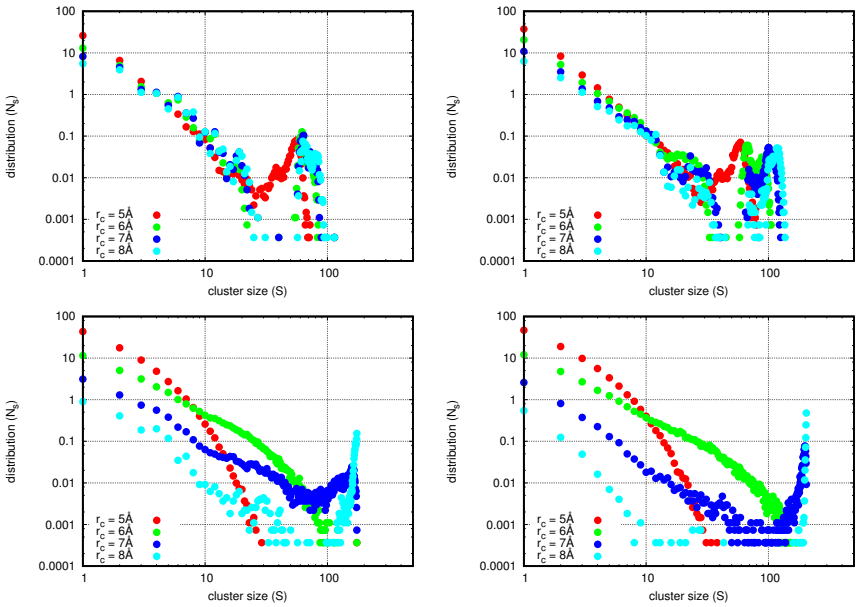

Figure 6: Cluster size distribution for (Top) DPPC and (Bottom) DOPC lipids without (left) and with (right) CHOL, using various cut-off distances.

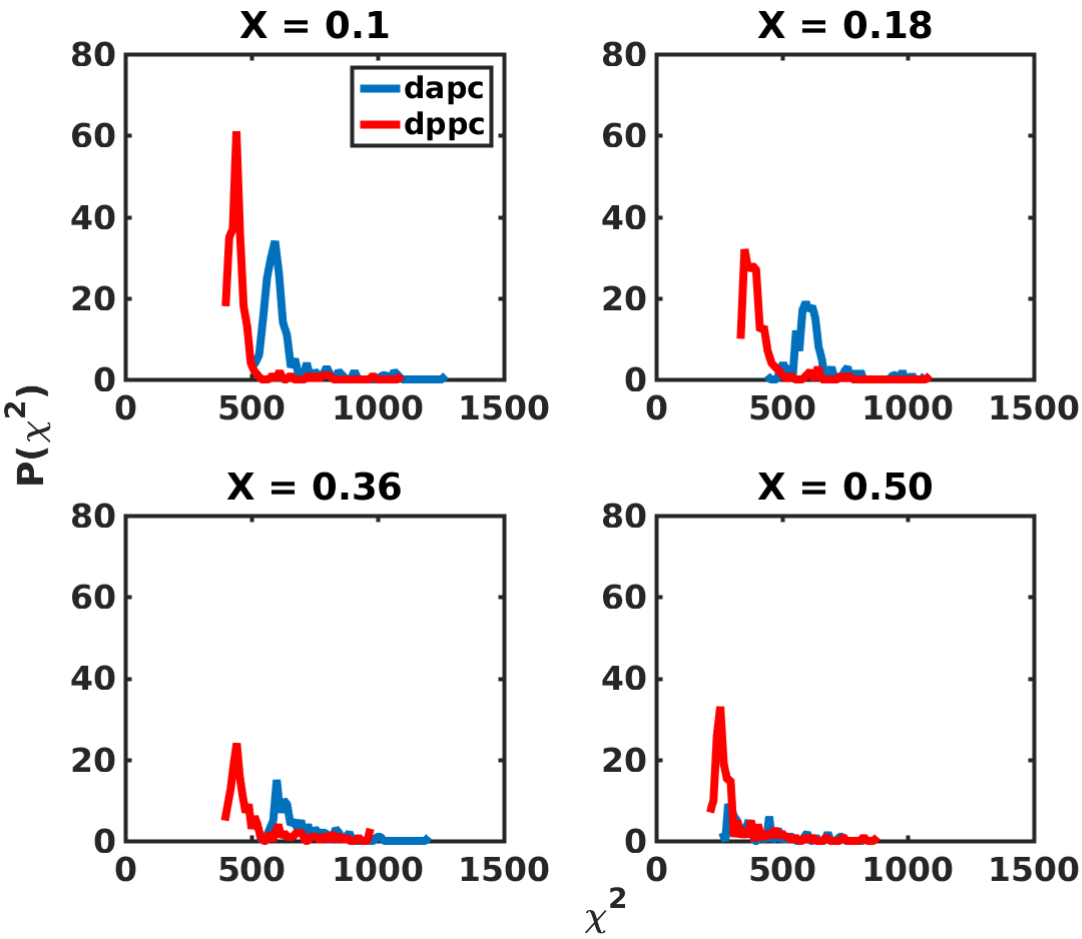

Figure 7: Probability distribution of χ^2 values of DAPC and DPPC lipid types for systems with increasing linactant concentrations shows that the overlap in the long tails increases linearly. This indicates that linactant break the domain boundary thus disrupting phase separation.

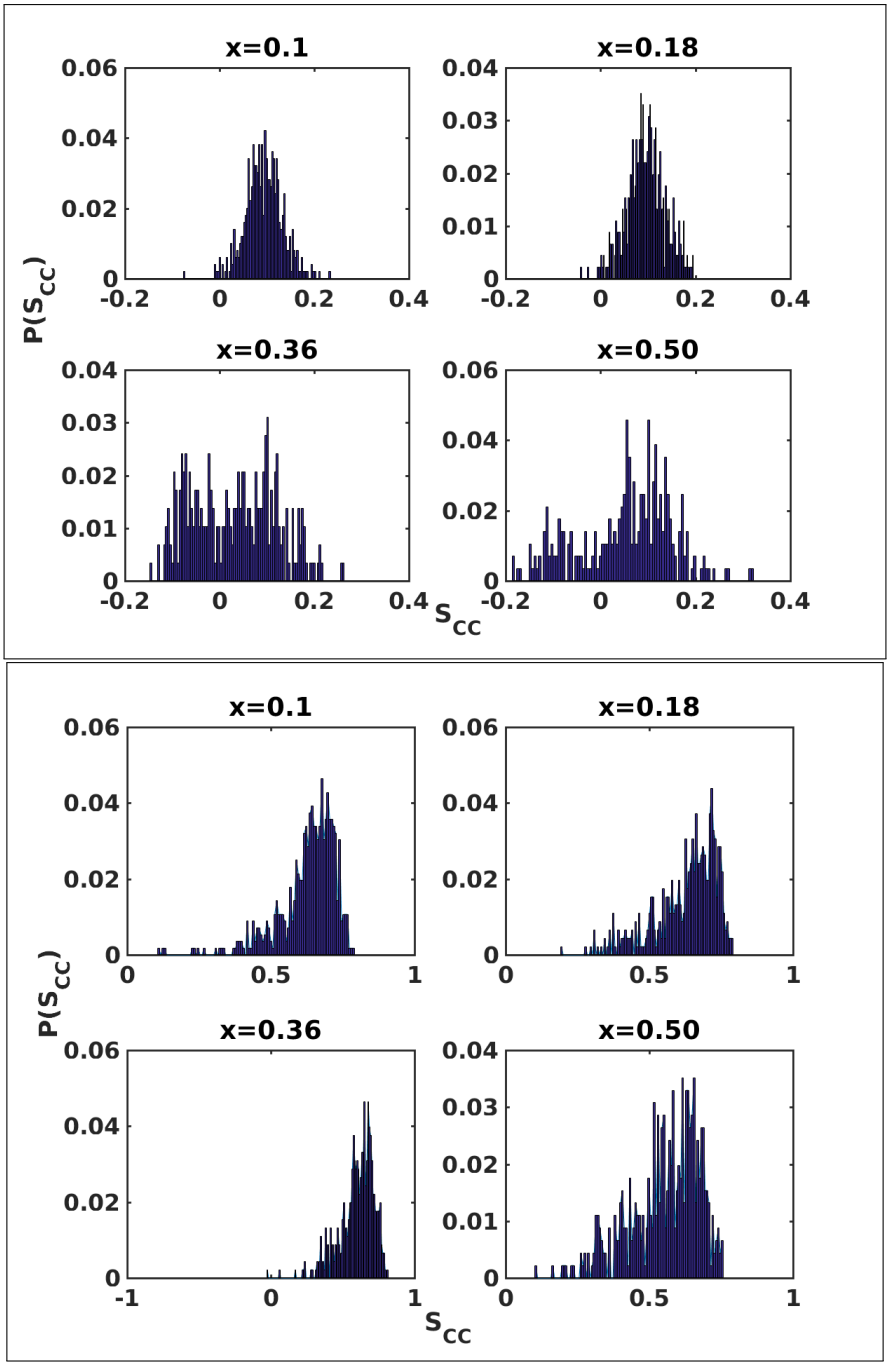

Figure 8: Probability distribution of tail order parameters for (Top) DAPC and (Bottom) DPPC lipids for different linactant ratios. Whereas the change in order parameter in DPPC lipids is not significant, the dispersion in order parameter values for DAPC increases with linactant ratio.